A numerical study on the performance of miniature thermoelectric cooler affected by Thomson effect

Wei-Hsin Chen [a,*], Chen-Yeh Liao [b], Chen-I Hung [b]

[a] *Department of Greenergy, National University of Tainan, Tainan 700, Taiwan, ROC*
[b] *Department of Mechanical Engineering, National Cheng Kung University, Tainan 701, Taiwan, ROC*

ARTICLE INFO

ABSTRACT

Miniature thermoelectric cooler (TEC) has been considered as a promising device to achieve effective cooling in microprocessors and other small-scale equipments. To understand the performances of miniature thermoelectric coolers, three different thermoelectric cooling modules are analyzed through a three-dimensional numerical simulation. Particular attention is paid to the influence of scaling effect and Thomson effect on the cooling performance. Two different temperature differences of 0 and 10 K between the top and the bottom copper interconnectors are taken into account. In addition, three different modules of TEC, consisting of 8, 20 and 40 pairs of TEC, are investigated where a single TEC length decreases from 500 to 100 μm with the condition of fixed ratio of cross-sectional area to length. It is observed that when the number of pairs of TEC in a module is increased from 8 to 40, the cooling power of the module grows drastically, revealing that the miniature TEC is a desirable route to achieve thermoelectric cooling with high performance. The obtained results also suggest that the cooling power of a thermoelectric cooling module with Thomson effect can be improved by a factor of 5–7%, and the higher the number of pairs of TEC, the better the improvement of the Thomson effect on the cooling power.

© 2011 Elsevier Ltd. All rights reserved.

1. Introduction

Over the last decade, the research and development of thermoelectric (TE) devices has attracted a great deal of attention because of their potential applications in green energy and energy management [1–4]. As a whole, TE devices in semiconductors can be classified into two different groups; one is the thermoelectric generator (TEG) [5–8] and the other the thermoelectric cooler (TEC) [9–16]. The function of the former is to convert heat into electricity through the Seebeck effect [17]; conversely, the purpose of the latter is to convert electricity into thermal energy through the Peltier effect [4,17,18]. Apart from the Seebeck and Peltier effects, the third thermoelectric effect, the Thomson effect, relating to reversible heating or cooling will also occur in a conductor when both the current and the temperature gradient are applied to the conductor [17,18].

As far as a TEC is concerned, as shown in Fig. 1a, each thermoelectric pair typically includes a p-type element (or semiconductor), an n-type element, a top copper interconnector and two bottom interconnectors. Once an electric current flows from the n-type semiconductor to the p-type one, heat will be absorbed on the cold side and delivered to the hot side, thereby implementing heat transport and cooling. In contrast to conventional heat pumps

and refrigerators, TEC possesses the advantages of direct energy conversion, high reliability, low maintenance, compactness, no moving parts causing vibration and no refrigerants [13]. In addition, the degree of cooling can be readily controlled by varying electrical current applied in the device, implying that the operation of cooling is highly flexible. Moreover, the input current can even be provided by TEG [19,20]. For these reason, TEC has been considered to a promising device applied in electronic, optoelectronic and bioanalytical devices, such as microprocessors, semiconductor lasers and DNA micro-arrays [14].

The performance of a thermoelectric material is usually evaluated using an index called the figure of merit (ZT). The index of ZT is a dimensionless parameter and it is defined by

$$ZT = \frac{\alpha^2}{\rho_e k} T \qquad (1)$$

In the preceding equation, α, T, ρ_e, k are the Seebeck coefficient, temperature (usually the room temperature), electrical resistivity and thermal conductivity, respectively [16,21,22]. A higher ZT value will lead to a better performance of a thermoelectric device. Because of this, a lot of efforts have been made to reach a higher figure of merit [17,23–27] by means of enlarging Seebeck coefficient, decreasing electrical resistivity and reducing thermal conductivity since it will lead to a better performance of a thermoelectric device.

* Corresponding author. Tel.: +886 6 2605031; fax: +886 6 2602205.
E-mail address: weihsinchen@gmail.com (W.-H. Chen).

Nomenclature

A	cross-sectional area of thermoelectric element (m^2)
COP	coefficient of performance (dimensionless)
E	electric field intensity ($V\,m^{-1}$)
G	ratio of the cross-sectional area to length of thermoelectric element (m)
I	electric current (A)
J	electric current density ($A\,m^{-2}$)
K	thermal conductance ($W\,K^{-1}$)
k	thermal conductivity ($W\,m^{-1}\,K^{-1}$)
L	length of thermoelectric element (m)
N	number of thermoelectric pairs (dimensionless)
P	supplied power (W)
$\dot{q}$	heat generation per unit volume ($W\,m^{-3}$)
q	heat flux ($W\,m^{-2}$)
Q_c	cooling power (W)
T	absolute temperature (K)
Z	thermoelectric figure-of-merit (K^{-1})

Greek letters

α	Seebeck coefficient ($V\,K^{-1}$)
β	Thomson coefficient ($V\,K^{-1}$)
Δ	temperature difference (K)
ρ	density ($kg\,m^{-3}$)
ρ_e	electrical resistivity ($\Omega\,m$)
ϕ	electric scalar potential (V)
ξ	the ratio of Thomson heat to the conduction heat ($=\beta I/K$)

Subscript

c	cold side
h	hot side
in	inside semiconductor
n	n-type
o	optimum
p	p-type
0	without Thomson effect
max	maximum

Seeing that TEC is likely to be employed for high cooling power density, resulting from easy integration with microelectronic components, recent partial interest in TEC has focused on the miniaturization of TEC size [12,28]. In the study of Chowdhury et al. [14], the viable chip-scale refrigeration technology by fabricating thin-film thermoelectric coolers was demonstrated. They mentioned that TEC had the potential to enable a wide range of currently thermally limited applications. Zhang et al. [15] reported that the cooling power of a TEC was inversely proportional to the thermoelectric element length; hence the change of the bulk TEC dimension was

thought of as an alternative strategy to achieve high cooling power density. Simons et al. [13], Sharp et al. [29] and Wu et al. [1] pointed out that the improvement of TEC could be realized by scaling the module size of the thermoelectric cooler downward. In the study of Chen et al. [30], the Thomson effect on the performance of TEG has been discussed and they highlighted the induced error in the predictions when the Thomson effect was neglected. Huang et al. [31,32] addressed that the performance of TEC could be improved not only by increasing the figure of merit of thermoelectric materials but also by taking the Thomson effect into account. Seifert et al.
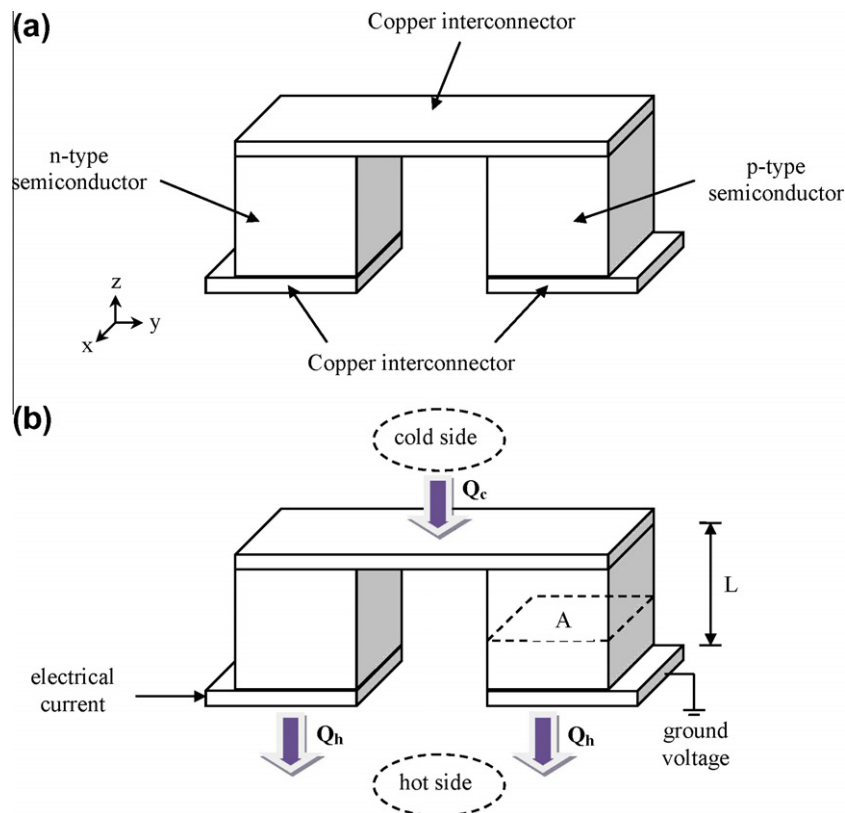

Fig. 1. Schematics of (a) geometry of a TEC and (b) heat flow in the TEC.

[33], Yamashita [34] and McCarty [35] examined the influence of temperature-dependent TE materials on the behavior of TECs.

In some studies introduced above [1,12–16,28,29], Fourier's heat conduction and Joule's heating have been considered; however, the Thomson effect was ignored in that the Seebeck coefficients were assumed to be constant. In other studies [30–35], though the Thomson effect has been regarded, the geometric miniaturization or scaling down effect on the performance of TEC was absent. For these reasons, the present study is intended to explore the performances of three different modules in which miniature thermoelectric coolers are installed. Particular emphasis is placed on the Thomson effect in association with the geometric scaling down upon the behavior of the thermoelectric cooling modules (TECMs). In the study, the ratio of cross-sectional area to length of a TE element will be fixed. Detailed performance and thermal behavior of the TECMs will be described below.

2. Mathematical formulation and modeling

2.1. Thermoelectric cooler and assumptions

Attention of this study is focused on the performances of three TECMs in which various numbers of TEC are embedded. The geometric unit of a TEC inside a module and its coordinate system are shown in Fig. 1a. As seen in Fig. 1a, the TEC comprises a p-type semiconductor (or element), an n-type semiconductor and three copper interconnectors. When the TEC is scaled down, the ratio of cross-sectional area to length of a TEC will be fixed and thereby the number of TEC in the module is increased. To simplify the physical problem, the following assumptions are adopted; they include: (1) the TECM is in steady-state; (2) the ratio of cross-sectional area

to length of a TEC is fixed; (3) heat loss from convection and radiation is ignored in that it is very small compared to the cooling power of the TECM; (4) contact resistance is disregarded; (5) the thermal conductivity and electrical resistivity are constant; and (6) the
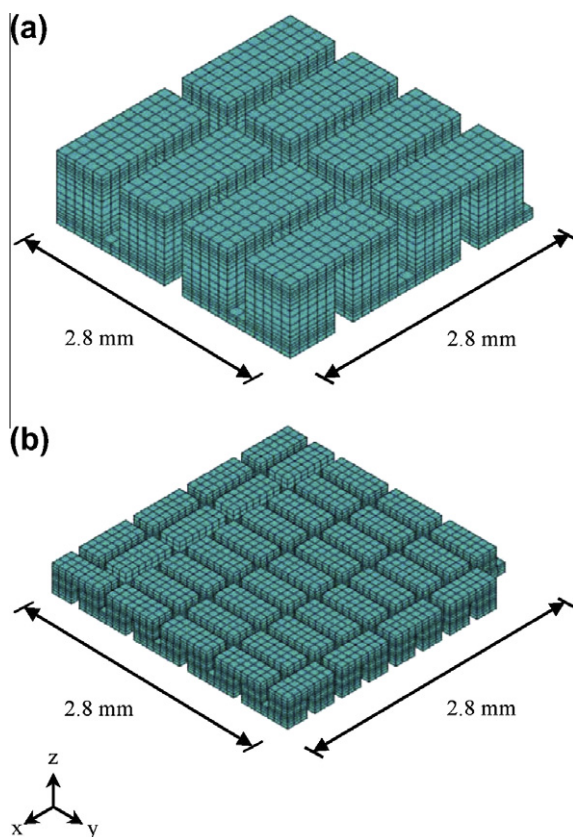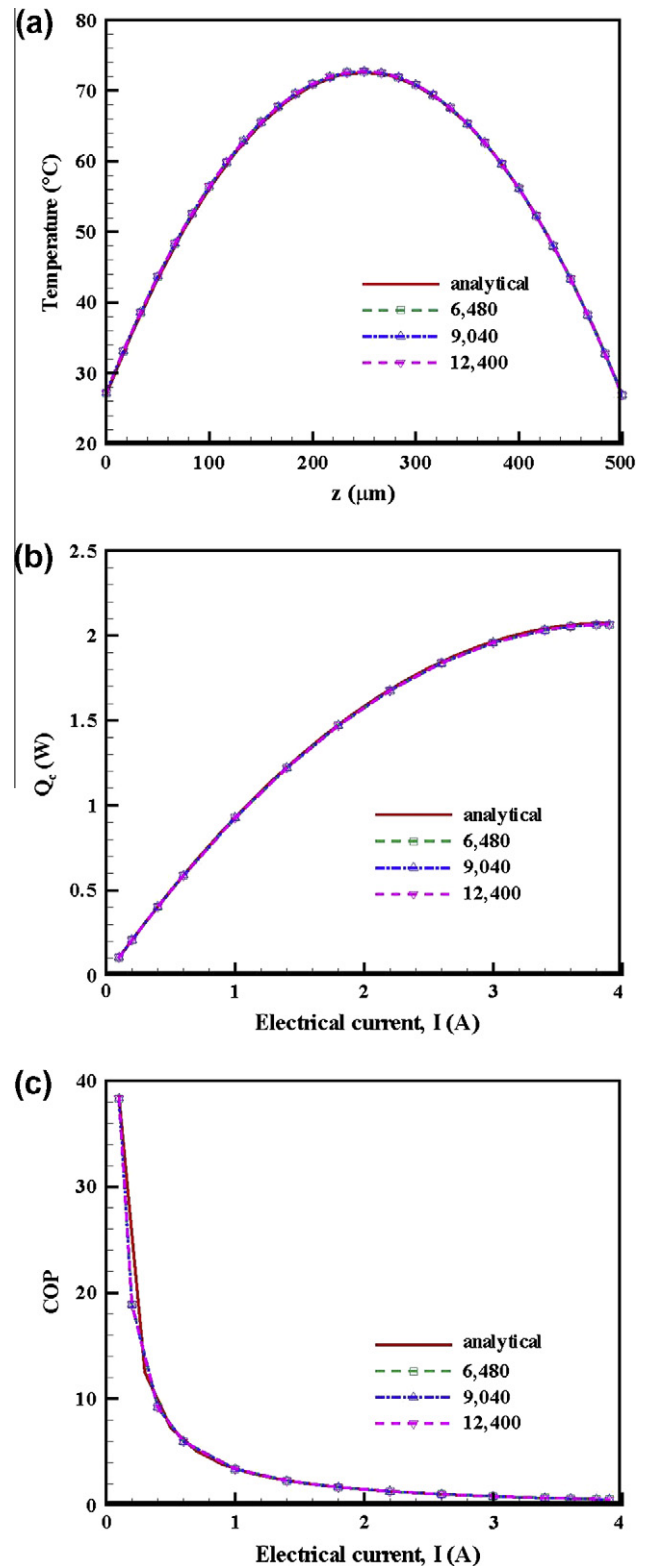

Fig. 3. Distributions of (a) temperature along the z-direction of the p-type TE element, (b) cooling power and (c) coefficient of performance for Module 1 at three different grid systems.

Fig. 2. Schematics of the grid system and the arrangement of TEC in a module with (a) 8 TECs (Module 1) and (b) 40 TECs (Module 3).

cross-sectional areas of a p-type element and an n-type element are equivalent.

2.2. Governing equations

In a thermoelectric analysis, the three-dimensional governing equations of heat flow in TEC at steady state can be cast into the following general form

$$\nabla \cdot \vec{q} = \dot{q} \tag{2}$$

In the foregoing equation, the heat flux vector $\vec{q}$ in terms of the electric current density vector $\vec{J}$ and Fourier's law $k\nabla T$ is expressed as the following:

$$\vec{q} = \alpha T \vec{J} - k\nabla T \tag{3}$$

$$\vec{J} = \frac{1}{\rho_e}(\vec{E} - \alpha \nabla T) \tag{4}$$

where $\vec{E} = -\nabla \phi$ is the electric field intensity vector and ϕ is the electric scalar potential. When substituting Eq. (3) into Eq. (2), the governing equations of heat flow becomes

$$\nabla \cdot (k\nabla T) - \nabla \cdot (\alpha T \vec{J}) + \dot{q} = 0 \tag{5}$$

The heat generation term $\dot{q}$ shown in the preceding equation includes the electric power $J \cdot E$ spent on Joule heating and on work against the Seebeck field $\alpha \nabla T$ [36]. In Eqs. (4) and (5), k, α and ρ_e are the thermal conductivity, Seebeck coefficient and electrical resistivity of a TE element, respectively. Furthermore, with the assumptions of constant material properties k and ρ_e, the temperature distribution in the interior of TEC can be described by a linear second-order differential equation as

$$k\nabla^2 T - \vec{J}\beta\nabla T + |\vec{J}|^2 \rho_e = 0 \tag{6}$$

where the temperature dependence of Seebeck coefficient has been taken into account to emphasize the Thomson effect since the Thomson coefficient is defined by

$$\beta = T\frac{d\alpha}{dT} \tag{7}$$

Physically, the terms appeared on the left-hand-side of Eq. (6) represent the conducted heat, Thomson heat and Joule's heat, respectively.

2.3. Boundary conditions

In the current study, two different temperature differences between the top and the bottom interconnectors are considered. Therefore, the temperatures of the top and the bottom interconnectors are given by

$$T(z = 0) = T_h \quad \text{and} \quad T(z = L) = T_c \tag{8}$$

In the meantime, heat loss along the side surfaces of the n-type and p-type semiconductors are ignored. This implies

$$\frac{\partial T}{\partial x} = 0 \quad \text{and} \quad \frac{\partial T}{\partial y} = 0 \tag{9}$$

2.4. Cooling power and coefficient of performance

When a TECM is executed, two important indexes are evaluated; one is the cooling power and the other the coefficient of performance (COP). The cooling power or heat pumped capacity (Q_c) of a TECM is defined as the net heat flow rate into the module from the cold side and it expressed as

$$Q_c = N(Q_\alpha - Q_p - Q_n) \tag{10}$$

where N is number of pairs of TEC in the module and the terms Q_α, Q_p and Q_n, standing for heat pumped rate due to the Peltier effects of the p-type and n-type semiconductors, heat transfer rates into
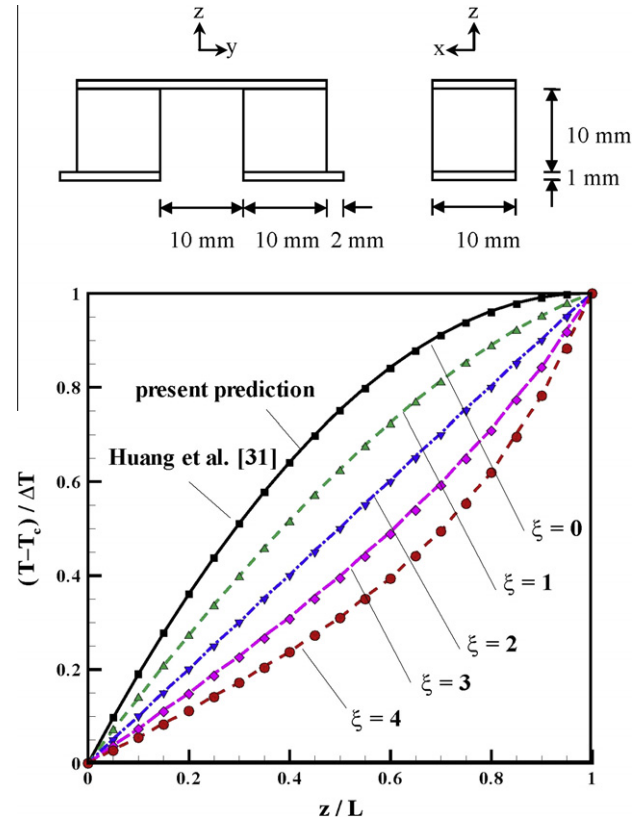

Fig. 4. Comparisons of temperature distribution along the z-direction of the p-type TE element.

Table 1
Physical sizes of single elements of semiconductors installed in three different modules.

Name	No. of TEC	Cross-sectional area A (m²)	Length L (m)	A/L (m)
Module 1	8	2.5×10^{-7}	5.0×10^{-4}	5.0×10^{-4}
Module 2	20	1.0×10^{-7}	2.0×10^{-4}	5.0×10^{-4}
Module 3	40	5.0×10^{-8}	1.0×10^{-4}	5.0×10^{-4}

Table 2
Properties of the TE element and copper interconnector [34,36,38].

Properties of p-type element	
Seebeck coefficient (V K⁻¹)	$-6.95 \times 10^{-10}(T - 300)^2 + 3.42 \times 10^{-7}(T - 300) + 2.207 \times 10^{-4}$
Thermal conductivity (W m⁻¹ K⁻¹)	1.472
Electrical resistivity (Ω m)	8.826×10^{-6}
Properties of n-type element	
Seebeck coefficient (V K⁻¹)	$1.04 \times 10^{-9}(T - 300)^2 - 1.25 \times 10^{-7}(T - 300) - 2.23 \times 10^{-4}$
Thermal conductivity (W m⁻¹ K⁻¹)	1.643
Electrical resistivity (Ω m)	8.239×10^{-6}
Properties of copper interconnector	
Seebeck coefficient (V K⁻¹)	6.5×10^{-6}
Thermal conductivity (W m⁻¹ K⁻¹)	400
Electrical resistivity (Ω m)	1.7×10^{-9}

the cold side from the p-type and n-type elements, respectively, are written as

$$Q_{\alpha} = (\alpha_p - \alpha_n)IT\big|_{z=L}, \quad Q_p = -k_p A \frac{dT_p}{dz}\bigg|_{z=L} \quad \text{and} \quad Q_n = -k_n A \frac{dT_n}{dz}\bigg|_{z=L} \tag{11}$$

With regard to the COP of a TECM, it means the ratio of cooling power to supplied power (P) and it is expressed as

$$COP = \frac{Q_c}{P} = \frac{Q_c}{I\Delta V} = \frac{Q_c}{Q_h - Q_c} \tag{12}$$

2.5. Numerical method and grid system

To predict the performances of TECMs with three-dimensional model, the commercial software ANSYS 12.0.1 was utilized to solve the governing equations in association with the boundary conditions. In the software, the finite element method in conjunction with the Galerkin procedure [36,37] was used to obtain the finite element equations.

As far as the grid system is concerned, the geometric structures and grid systems of the TECMs with 8 and 40 TECs are displayed in Fig. 2a and b, respectively. When the TECM with 8 TECs was calculated, three different grid systems with total elements of 6480, 9040 and 12,400 are tested and compared with each other to seek an appropriate grid system. In the three grid systems, the distributions of temperature along the z-direction of the p-type semiconductor (Fig. 3a), cooling power (Fig. 3b) and COP (Fig. 3c) versus electric current are shown in Fig. 3 where the temperatures at the hot side and the cold side are identical (27 °C) and the input current is 3.9 A. The Seebeck coefficients of the n-type and the p-type elements are set as $-223.0\ \mu V\ K^{-1}$ and $220.7\ \mu V\ K^{-1}$, respectively. It can be seen that the discrepancy among the curves

with the three grid systems are almost imperceptible, implying that the grid system with 9040 elements is proper for simulation. Moreover, the comparisons between the simulations and the analytical solutions [17,18] in the absence of Thomson effect reflect that the numerical method is accurate. After a series of tests, the grid systems of 9040, 11,648 and 13,287 elements are adopted for the predictions of TECMs with 8, 20 and 40 TECs, respectively. To further validate the numerical method in the presence of Thomson effect, the temperature profiles in a TEC at various Thomson coefficients are predicted and displayed in Fig. 4 where the Thomson coefficients are assumed to be constant. The physical size of the TEC is also embedded in Fig. 4. From the comparisons with the results of Huang et al. [31], it is obvious that the present predictions almost overlap the results of Huang et al. [31]. Accordingly, the developed numerical method enables us to predict the performances of TECMs accurately.

3. Results and discussion

As mentioned above, three different TECMs are taken in account where 8, 20 and 40 TECs are individually embedded in a module. To provide a basis for investigation, the area of the module is fixed at $2.8 \times 2.8\ mm^2$ and the temperature of the hot side (T_h) is set at 300 K. Moreover, the ratio of cross-sectional area (A) to length (L) of an element is also constant. As a consequence, when 8, 20 and 40 TECs are assembled as a module, the length of the element is reduced from 500 to 100 μm. Detailed geometric sizes of the three modules are listed in Table 1. To emphasize the Thomson effect on the performances of the TECMs, the Seebeck coefficients of the p-type and n-type semiconductors are expressed by quadratic functions of temperature [34]. Rest properties such as thermal conductivity and electrical resistivity are assumed constant. The values of Seebeck coefficient, thermal conductivity and electrical
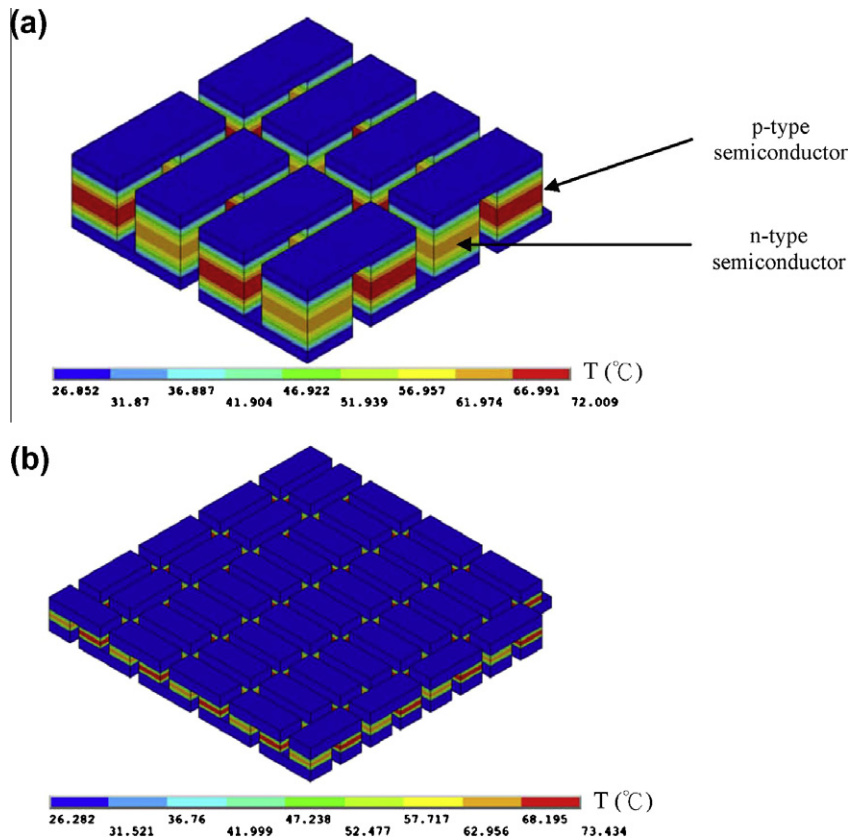

Fig. 5. Isothermal contours of (a) Module 1 and (b) Module 3 with Thomson effect ($\Delta T = 0$ K).

resistivity are given in Table 2. Under the aforementioned conditions, the value of figure of merit (ZT) is 1.1 at 300 K. In addition, two different temperature differences between the hot side and the cold side (i.e. $\Delta T = 0$ and 10 K) are considered. In the following discussion, the modules with 8, 20 and 40 TECs are referred to as Module 1, Module 2 and Module 3, respectively.

3.1. Temperature distribution

First of all, the isothermal contours of Module 1 and Module 3 at the condition of $\Delta T = 0$ K are demonstrated in Fig. 5. On account of the electrical resistances of the p-type and n-type semiconductors, Joule's heat is generated and accumulated inside the semiconductors once electrical current passes through the TEC. The electrical resistivity of the p-type element is higher than that of the n-type one (Table 2) so that the temperature in the former is higher than that in the latter. Detailed temperature distributions inside the p-type and the n-type semiconductors are plotted in Fig. 6 and Fig. 7, respectively. Basically, for the case of $\Delta T = 0$ K in Module 1 where the current is 3.9 A, the maximum temperature is around 73 °C and the Thomson effect just deviates the temperature profile a bit (Fig. 6a). In Module 3, the current density is higher; this results in a higher temperature distribution and the maximum temperature is lifted to 76 °C (Fig. 6b). In regard to the temperature profile inside the n-type semiconductor with the condition of $\Delta T = 0$ K, the maximum temperatures in Module 1 and Module 3 are 65 (Fig. 7a) and 68 °C (Fig. 7b), respectively. It is noted that the temperature distribution in the n-type semiconductor is hardly affected by the Thomson effect. Therefore, the Thomson effect on the p-type semiconductor is larger than on the n-type one. Fig. 8 further presents the profiles of the maximum temperature difference (i.e. $\Delta T_{in,\,max}$) in the p-type and the n-type semiconductors at the three modules. Apparently, the maximum temperature difference rises as the number of TEC in a module goes up or the size of TEC goes down. Moreover, the maximum temperature difference in the p-type semiconductor is larger than that in the n-type one around 7–8 °C.

3.2. Cooling power of TECM

Upon inspection of the cooling power expressed in Eq. (10), it is recognized that the performance of a TECM comes from three fac-
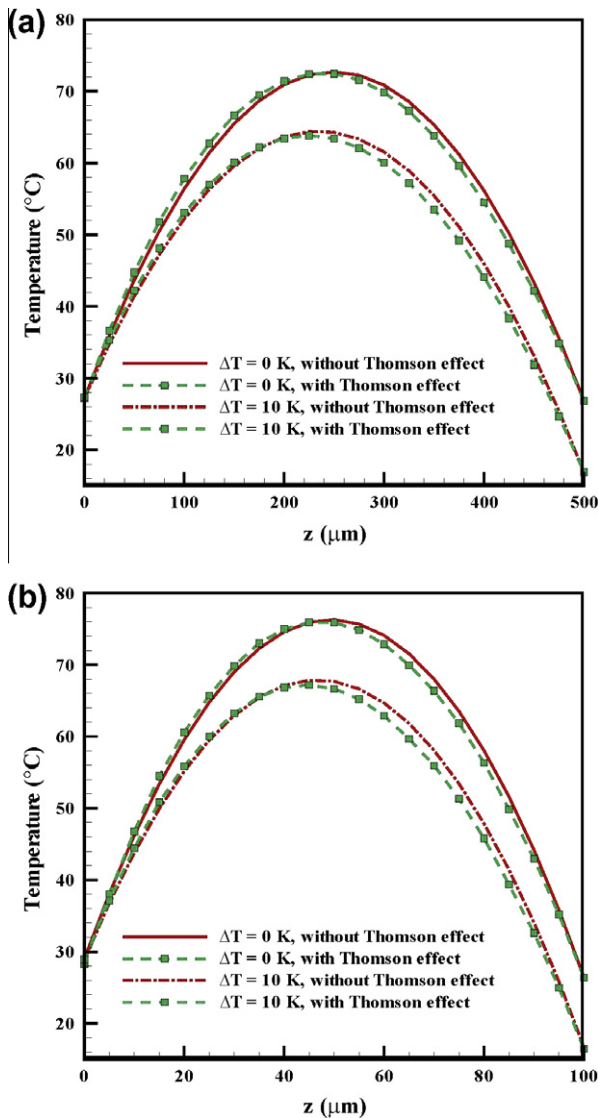

Fig. 6. Temperature distributions along the z-direction of the p-type semiconductor in (a) Module 1 and (b) Module 3 at $\Delta T = 0$ K ($I = 3.9$ A) and $\Delta T = 10$ K ($I = 3.75$ A).
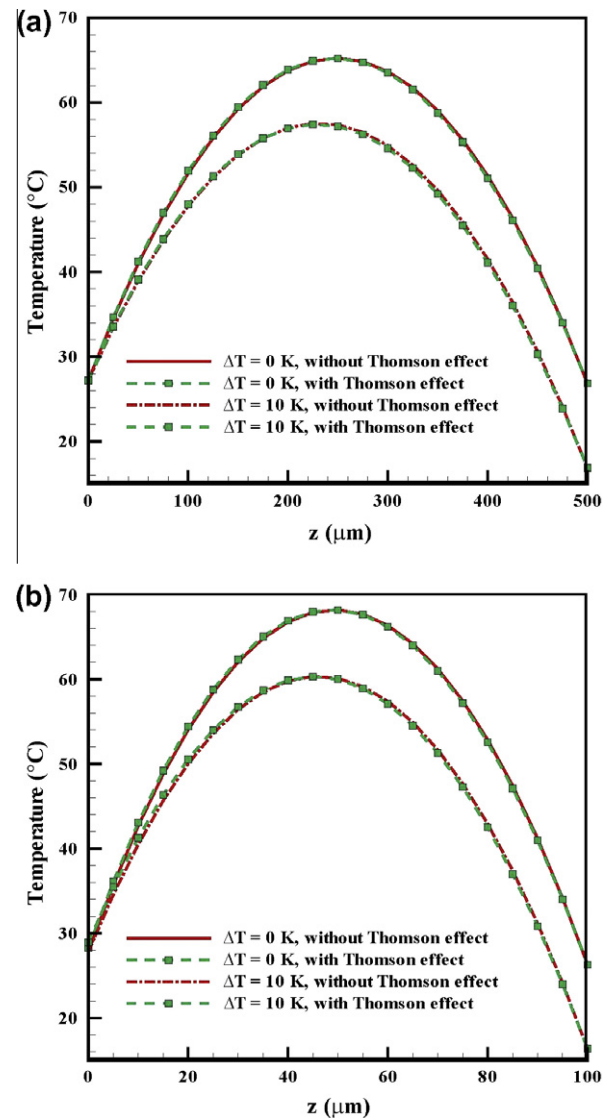

Fig. 7. Temperature distributions along the z-direction of the n-type semiconductor in (a) Module 1 and (b) Module 3 at $\Delta T = 0$ K ($I = 3.9$ A) and $\Delta T = 10$ K ($I = 3.75$ A).

tors; they are Q_α, Q_p and Q_n. Physically, Q_α represents heat pumped due to the Peltier effects of the p-type and n-type semiconductors and it is considered as a heat sink to the cold-side interconnector. On the contrary, Q_p and Q_n designate heat transferred into the cold-side interconnector stemming from Joule's heat and the temperature difference; therefore, the two terms behave as the heat source to the cold-side interconnector. To figure out the roles played by the three terms on the performances of the three modules, the distributions of the three terms with respect to current in the absence of Thomson effect are sketched in Fig. 9. In examining the distributions shown in Fig. 9a–c, it can be found that the differences between the three figures are quite small, implying that the three terms Q_p and Q_n to Q_α are independent of module or number of pairs of TEC. Accordingly, from Eq. (10) it is known that the cooling power of a TECM is proportional to the number of pairs of TEC embedded in a module [1,13,29]. Moreover, it suggests that Q_α is much larger than Q_p and Q_n, implying that the first term is the dominant mechanism, so that heat can be pumped from the cold side. However, it should be mentioned that ratio of the summation of Q_p and Q_n to Q_α is linearly proportional to the current. It follows

that the two heat source terms become more and more important as the current increases. Consequently, from the viewpoint of heat sink and heat source, a lower current is conducive to distinguishing the Peltier effect. Meanwhile, despite the discrepancy in the temperature distribution in the p-type and n-type semiconductors (Figs. 6 and 7), the difference between Q_p and Q_n is slight. This reflects that the heat sources played by the p-type and n-type semiconductors on the cold side are almost equivalent.
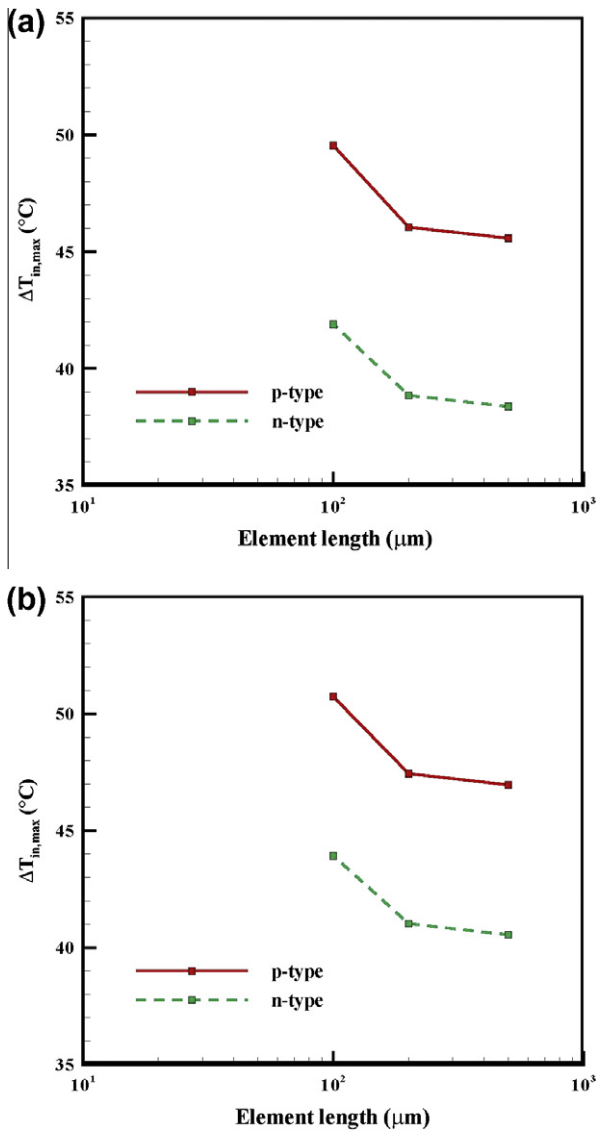

Fig. 8. Profiles of maximum temperature difference inside the TE elements with respect to element length at ΔT = (a) 0 K (3.9 A) and (b) 10 K (3.75 A) with Thomson effect.
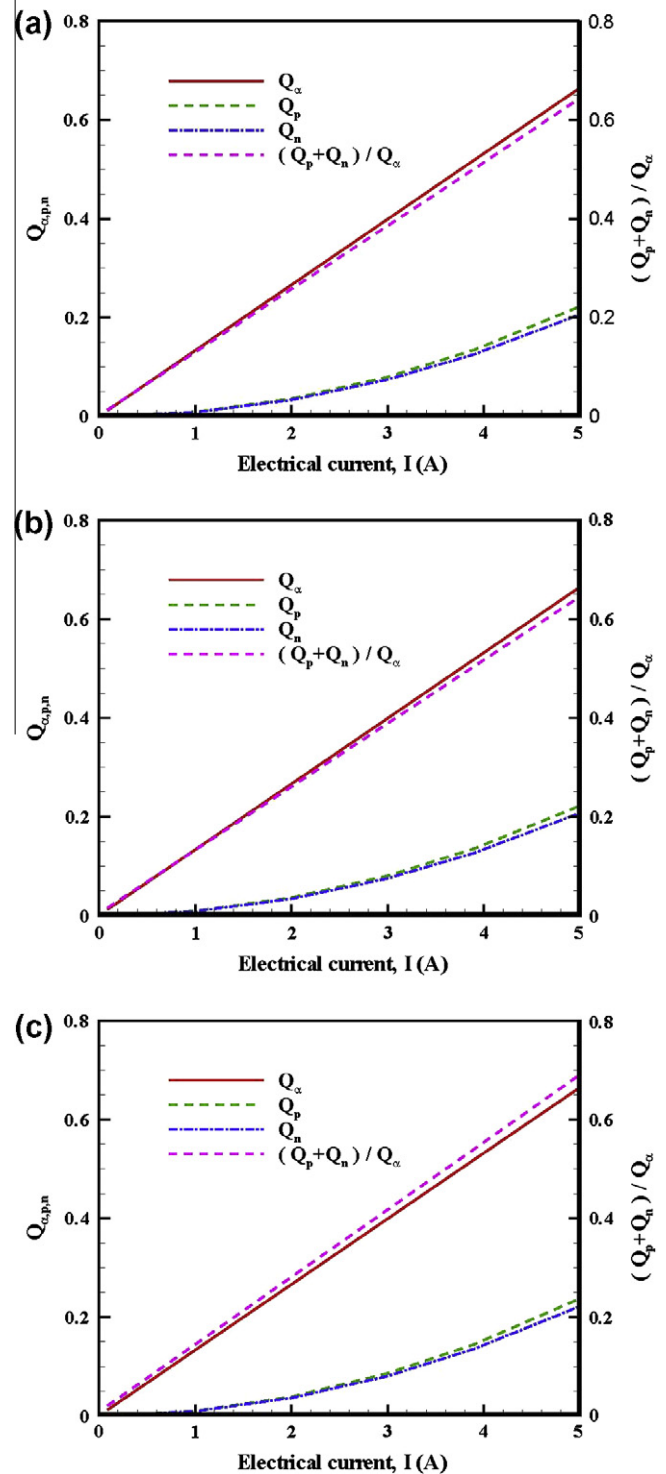

Fig. 9. Distributions of Q_α, Q_p and Q_n of (a) Module 1, (b) Module 2 and (c) Module 3 with respect to electrical current without Thomson effect (ΔT = 0 K).

3.3. Influence of Thomson effect

The distributions of cooling power (Q_c) and the ratio of Q_c in the presence and absence of Thomson effect as well as COP of the three different modules without temperature difference between the hot side and the cold side (i.e. $\Delta T = 0$) are demonstrated in Fig. 10. A comparison between the curves with and without Thomson effect indicates that the Thomson effect is able to enhance the cooling power of a module to a certain extent (Fig. 10a), regardless of what

number of pairs of TEC inside the module. Obviously, the higher the current, the more significant the improvement of the Thomson effect on the cooling power. Similarly, the more TEC embedded in a module, the more pronounced the Thomson effect. Considering the three modules with Thomson effect, the optimal current for the cooling power occurs at 4.2 A, whereas it exhibits at 3.9 A in the absence of the Thomson effect. For the current of 3.9 A with the Thomson effect, the increments of the cooling power in Modules 1, 2 and 3 are 5.73%, 5.84% and 6.51%, respectively, in contrast to those without the Thomson effect (Fig. 10b). In examining
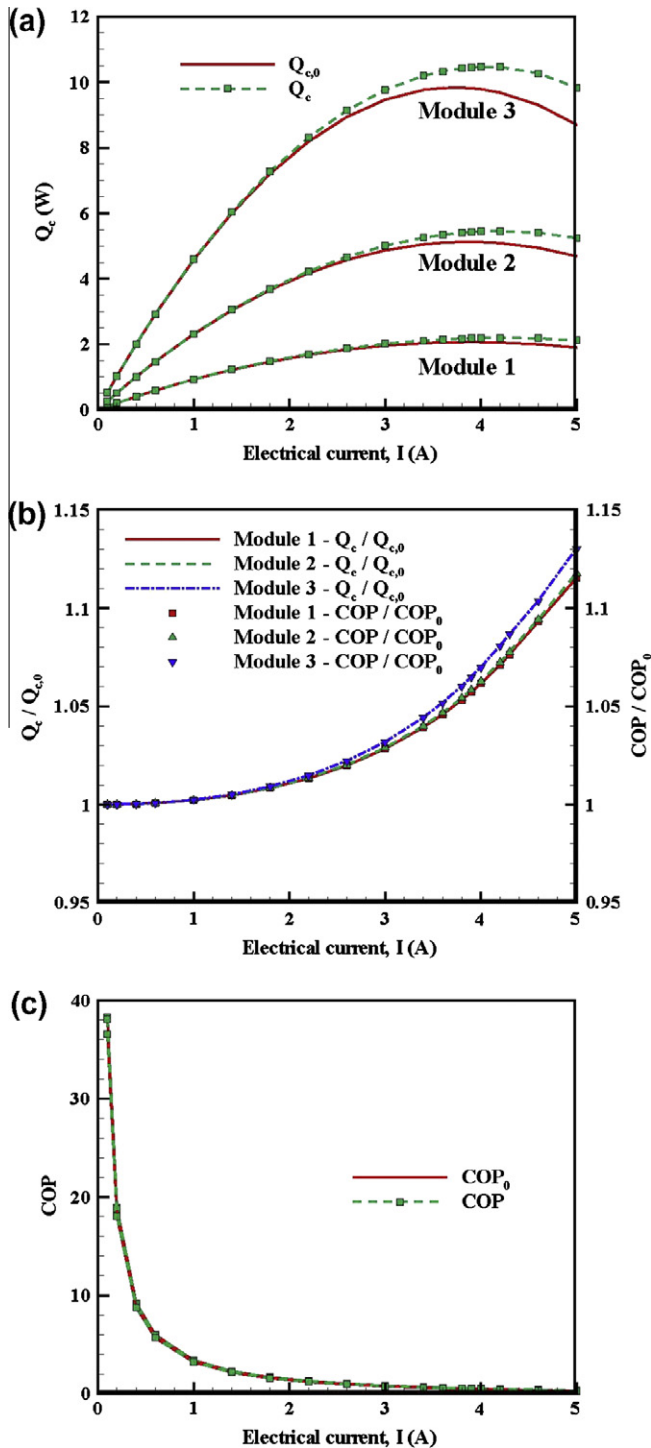

Fig. 10. Distributions of (a) cooling power, (b) the ratio of cooling power in the presence and absence of Thomson effect and (c) COP of three modules at $\Delta T = 0$ K.

Fig. 11. Distributions of (a) cooling power, (b) the ratio of cooling power in the presence and absence of Thomson effect and (c) COP of three modules at $\Delta T = 10$ K.
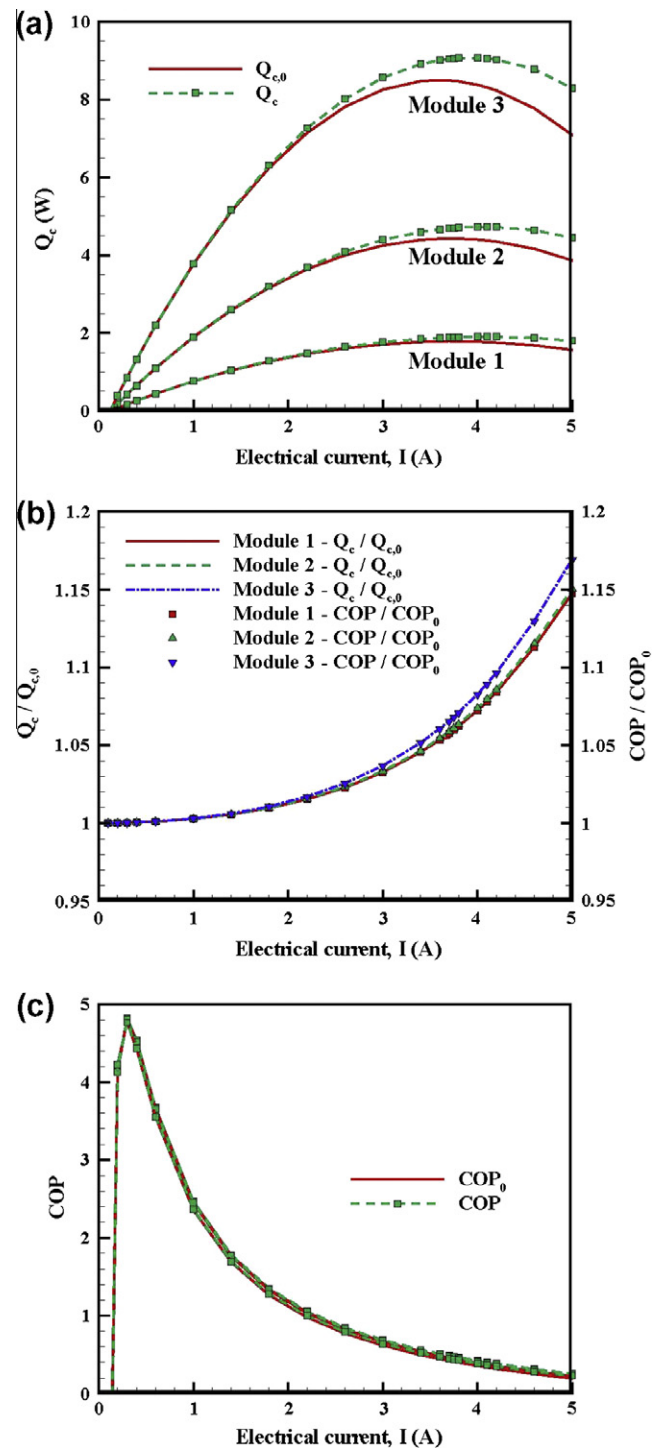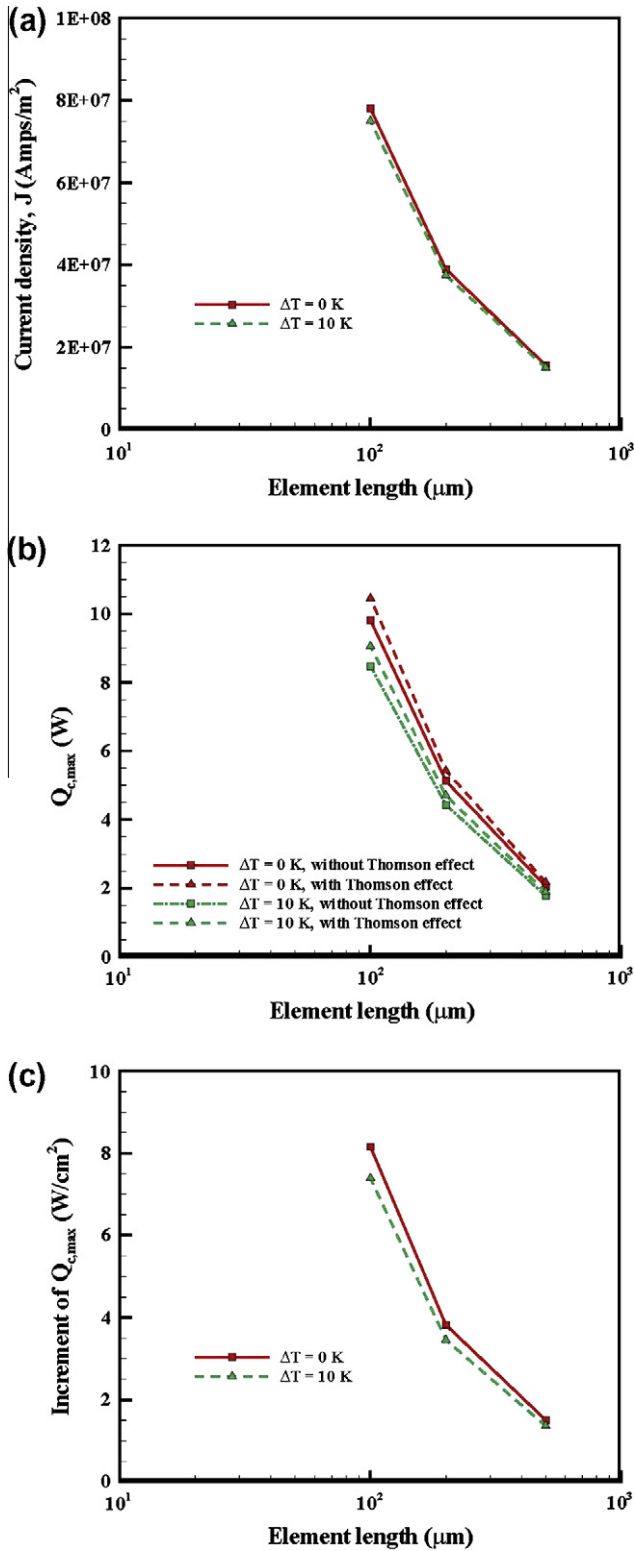
Fig. 12. Distributions of (a) current density, (b) maximum cooling power and (c) increment of the maximum cooling power due to Thomson effect with the conditions of ΔT = 0 and 10 K.

Fig. 10c, it can be found that Thomson effect also plays the same part in improving COP and this is consistent with the study of Huang et al. [31]. Fig. 10a also depicts that increasing the number of TEC in a module increases the cooling power dramatically. For example, corresponding to Modules 1, 2 and 3 with Thomson ef-

fect, the cooling powers at the electrical current of 4.2 A are 2.20, 5.46 and 10.47 W, respectively. Accordingly, it is figured out that miniaturizing a TEC by scaling down its size and increasing the number of TEC in a module is a feasible mean to intensify the cooling power of the module.

With the condition of temperature difference of 10 K, it can be seen that the curves of cooling power shown in Fig. 11a are somewhat lower than those shown in Fig. 10a, revealing that the cooling powers of the modules are abated slightly when a temperature difference exists between the hot side and the cold side. This arises from the fact that the temperature difference will induce conductive heat transfer, which is against the performance of cooling and thereby lessens the cooling power. The optimal currents with and without Thomson effect develop at 4.1 and 3.75 A, respectively, which is also slightly lower than those (i.e. 4.2 and 3.9 A) without temperature difference (Fig. 10a). With the current of 3.75 A, the increments of cooling power from Thomson effect in Modules 1, 2 and 3 are 6.00%, 6.12% and 6.83%, respectively (Fig. 11b). Furthermore, after comparing the curves between Figs. 10c and 11c it can be found that increasing temperature difference between the hot side and the cold side will facilitate the influence of Thomson effect as well,. Even though the enhancement of Thomson effect with increasing current, it should be addressed that one is unable to increase current too high in that there exists an optimal current of cooling power, as shown in Figs. 10a and 11a. Unlike the curves shown in Fig. 10c, it is of interest that the curves of COP are characterized by a maximum distribution and the maximum value of COP is 4.84 (Fig. 11c). The maximum value exhibits at the current of 0.292 A and it is independent of the number of pairs of TEC in a module. This can be explained by the following equation:

$$COP = \frac{(\alpha_p - \alpha_n)IT_c - 0.5I^2R - K\Delta T}{(\alpha_p - \alpha_n)I\Delta T + I^2R} \tag{13}$$

When one differentiates the foregoing equation, the maximum COP featured at 0.292 A is thus obtained.

Fig. 12a shows the profiles of current density at the two different temperature differences, whereas the profiles of the maximum cooling power corresponding to Figs. 10a and 11a are displayed in Fig. 12b. While scaling down the TEC in a module, the current density grows markedly (Fig. 12a). This leads to the pronounced growth in the maximum cooling power. The enhancement of Thomson effect on the maximum cooling power is also clearly observed (Fig. 12b). The increment in the maximum cooling power density stemming from Thomson effect is further examined in Fig. 12c. The figure depicts that the cooling power density can be increased up to 8 W cm^{-2} as Module 3 is employed.

4. Conclusions

The characteristics of thermal behavior and cooling power of three different TECMs have been investigated numerically with the aim to recognize the performance of miniature TEC in the presence/absence of Thomson effect. Three different modules by individually embedding 8, 20 and 40 TECs in a module have been taken into account. With the condition of fixed ratio between the cross-sectional area and the length of a TEC, the predictions indicate that the cooling power and COP of the module are increased notably when TECs inside a module are scaled down. This reflects that miniaturizing TEC size and increasing the number of TEC is an appropriate route to enhance the heat pump capacity of a TECM for cooling. The results also indicate that heat pumped or heat sink due to the Peltier effect is linearly proportional to the electrical current; however, two heat source terms stemming from Joule's

heat also grow. As a result, the three terms are independent of module or number of pairs of TEC. A maximum cooling power can be identified at a certain electrical current, depending on the Thomson effect and the temperature difference between the hot side and the cold side. As a whole, the optimal current for the cooling of a module in the presence of Thomson effect at $\Delta T = 0$ K develops at 4.2 A, whereas it occurs at 4.1 A for the case of $\Delta T = 10$ K, regardless of which module is utilized. The cooling power of a thermoelectric cooling module with Thomson effect can be improved by a factor of 5–7% in the investigated modules, and an increase in the number of pairs of TEC intensifies the improvement of the Thomson effect on the cooling power. Though an increase in the number of pairs of TEC is conducive to the improvement of Thomson effect on the cooling power, this leads to a decrease in the size of TEC due to the scaling effect. Once the size is reduced to a certain extent, the difficulty in the manufacture of TEC will be encountered. Besides, increasing the number of pairs significantly increases the current density. The induced Joule's heating may damage the TEC module. Accordingly, it should be illustrated that the number of pairs of TEC in a module is subject to the manufacturing techniques and practical applications. Therefore, a practical insight into the design of miniature TEC has been provided in the present study which is conducive to the applications of TEC.

Acknowledgements

References

[1] Wu KH, Hung CI. Thickness scaling characterization of thermoelectric module for small-scale electronic cooling. J Chin Soc Mech Eng 2009;30:475–81.
[2] Pan Y, Lin B, Chen J. Performance analysis and parametric optimal design of an irreversible multi-couple thermoelectric refrigerator under various operating conditions. Appl Energy 2007;84:882–92.
[3] van Sark WHJHM. Feasibility of photovoltaic – thermoelectric hybrid modules. Appl Energy 2011;88:2785–90.
[4] Gurevich YG, Logvinov GN. Physics of thermoelectric cooling. Semicond Sci Technol 2005;20:R57–64.
[5] Chen L, Li J, Sun F, Wu C. Performance optimization of a two-stage semiconductor thermoelectic-generator. Appl Energy 2005;82:300–12.
[6] Gou X, Xiao H, Yang S. Modeling, experimental study and optimization on low-temperature waste heat thermoelectric generator system. Appl Energy 2010;87:3131–6.
[7] Hsu CT, Huang GY, Chu HS, Yu B, Yao DJ. Experiments and simulations on low-temperature waste heat harvesting system by thermoelectric power generators. Appl Energy 2010;88:1291–7.
[8] Chen M, Lund H, Rosendahl LA, Condra TJ. Energy efficiency analysis and impact evaluation of the application of thermoelectric power cycle to today's CHP systems. Appl Energy 2010;87:1231–8.
[9] Yamashita O. Effect of temperature dependence of electrical resistivity on the cooling performance of a single thermoelectric element. Appl Energy 2008;85:1002–14.
[10] Chen L, Gong J, Shen L, Sun F, Wu C. Theoretical analysis and experimental confirmation for the performance of thermoelectric refrigerator. J Non-Equilib Thermodyn 2001;26:85–92.
[11] Luo J, Chen L, Sun F, Wu C. Optimum allocation of heat transfer surface area for cooling load and COP optimization of a thermoelectric refrigerator. Energy Convers Manage 2003;44:3197–206.
[12] Lee KH, Kim OJ. Analysis on the performance of the thermoelectric micro-cooler. Int J Heat Mass Transfer 2007;50:1982–92.
[13] Simons RE, Ellsworth MJ, Chu RC. An assessment of module cooling enhancement with thermoelectric coolers. ASME J Heat Transfer 2005;127:76–84.
[14] Chowdhury I, Prasher R, Lofgreen K, Chrysler G, Narasimhan S, Mahajan R, et al. On-chip cooling by superlattice-based thin-film thermoelectric. Nat Nanotechnol 2009;4:235–8.
[15] Zhang Y, Shakouri A, Zeng G. High-power-density spot cooling using bulk thermoelectrics. Appl Phys Lett 2004;85:2977–9.
[16] Abramzon B. Numerical optimization of the thermoelectric cooling devices. ASME J Electron Packag 2007;129:339–47.
[17] Rowe DM. Thermoelectric Handbook: Macro to Nano. 1st ed. CRC; 2006.
[18] Chen G. Nanoscale Energy Transport and Conversion. Oxford University; 2005.
[19] Meng F, Chen L, Sun F. Performance optimization for two-stage thermoelectric refrigerator system driven by two-stage thermoelectric generator. Cryogenics 2009;49:57–65.
[20] Meng F, Chen L, Sun F. Performance analysis for two-stage TEC system driven by two-stage TEG obeying Newton's heat transfer law. Math Comput Modell 2010;52:586–95.
[21] Mahan GD. Figure of merit for thermoelectric. J Appl Phys 1989;65:1578–83.
[22] Ioffe AF. Semiconductor Thermoelements and Thermoelectric Cooling. 1st ed. London: Info-search Ltd.; 1957.
[23] Fleurial JP. New Thermoelectric Materials and Devices: New Challenges. UCLA; 1997.
[24] Venkatasubramanian R, Siivola E, Colpitts T, O'Quinn B. Thin-film thermoelectric devices with high room-temperature figures of merit. Nature 2001;413:597–602.
[25] Cahill DG, Goodson K, Majumdar A. Thermomertry and thermal transport in micro/nanoscale solid-state devices and structures. J Heat Transfer 2002;124:223–41.
[26] Zhao XB, Ji XH, Zhang YH, Zhu TJ, Tu JP, Zhang XB. Bismuth telluride nanotubes and the effects on the thermoelectric properties of nanotube-containing nanocomposites. Appl Phys Lett 2005;86:062111-111–1-113.
[27] Poudel B. High-thermoelectric performance of nanostructured bismuth antimony telluride bulk alloys. Science 2008;320:634–8.
[28] Semenyuk V. Miniature thermoelectric modules with increased cooling power. In: 25th international conference on thermoelectrics; 2006.
[29] Sharp J, Bierschenk J, Lyon Jr HB. Overview of solid-state thermoelectric refrigerators and possible applications to on-chip thermal management. Proc IEEE 2006;94:1602–12.
[30] Chen J, Yan Z, Wu L. The influence of Thomson effect on the maximum power output and maximum efficiency of a thermoelectric generator. J Appl Phys 1996;79:8823–8.
[31] Huang MJ, Yen RH, Wang AB. The influence of the Thomson effect on the performance of a thermoelectric cooler. Int J Heat Mass Transfer 2005;48:413–8.
[32] Huang MJ, Chou PK, Lin MC. Thermal and thermal stress analysis of a thin-film thermoelectric cooler under the influence of the Thomson effect. Sensors Actuat A 2006;126:122–8.
[33] Seifert W, Ueltzen M, Muller E. One-dimensional modeling of thermoelectric cooling. Phys Status Solidi A – Appl Res 2002;194:277–90.
[34] Yamashita O. Effect of linear and non-linear components in the temperature dependences of thermoelectric properties on the cooling performance. Appl Energy 2009;86:1746–56.
[35] McCarty R. A comparison between numerical and simplified thermoelectric cooler models. J Electron Mater 2010;39:1842–7.
[36] Antonova EE, Looman DC. Finite elements for thermoelectric device analysis in ANSYS. In: 24th International conference on thermoelectrics; 2005.
[37] Silvester PP, Ferrari RL. Finite Elements for Electrical Engineers. Cambridge University; 1996.
[38] ANSYS Release 12.0.1 Documentation, ANSYS Inc.; 2010.